

Magnetoresistance properties of granular nanowires composed of carbon nanoparticles embedded in a Co matrix

J.-E. Wegrowe,* A. Sallin, A. Fábíán, A. Comment, J.-M. Bonard, and J.-Ph. Ansermet
Institut de Physique Expérimentale, Ecole Polytechnique Fédérale de Lausanne, CH-1015 Lausanne, Switzerland
 (Received 28 May 2001; published 30 November 2001)

Spin-dependent transport was studied in granular nanowires composed of magnetic and nonmagnetic nanoparticles embedded in a Co matrix. At low temperature, giant magnetoresistance (GMR) and tunnelinglike magnetoresistance (TMR) appear. GMR and TMR-like magnetoresistance are identified by the temperature and bias voltage dependence of the resistivity and the temperature dependence of the magnetoresistance. Electron microscopy observations suggest also that the percolation threshold of the particles in the wire triggers the transition from diffusive to hopping transport. The magnetoresistance behavior is very similar for both Ohmic and non-Ohmic transport. The origin of the magnetoresistance is ascribed to the presence of constrained magnetic walls pinned between the nanoparticles.

DOI: 10.1103/PhysRevB.65.012407

PACS number(s): 75.60.Ch, 75.70.Pa, 72.15.Gd

Diffusive and nondiffusive spin transport of conduction electrons are responsible for various types of magnetoresistance phenomena. Giant magnetoresistance (GMR) is measured in metal/ferromagnet multilayers,^{1,2} while tunneling magnetoresistance (TMR) is measured in non-Ohmic ferromagnet/insulating/ferromagnet multilayers.³ Both effects can also be observed in granular systems, with ferromagnetic grains embedded in a nonmagnetic matrix that is either metallic for GMR measurements^{4,5} or nonmetallic for TMR measurements.⁶⁻⁸ In usual granular systems, magnetic nanoparticles are dispersed in a nonmagnetic matrix, metallic (e.g., Ag, Au, Cu, ...) or insulating (e.g., SiO₂, Al₂O₃, ...).⁹

Granular systems give access to GMR and TMR measurements in disordered structures. It was observed that the two types of magnetoresistance (GMR and TMR) were surprisingly similar,⁷ considering that the electronic transport mechanisms are totally different. This similarity was observed in the amplitude of the magnetoresistance and in its dependence on the magnetic field and density of the magnetic material. It was also shown that the magnetoresistance does not depend on the volume of the magnetic nanoparticles in the matrix and is due to interface scattering.⁹ Furthermore, recent observations^{10,11} show that very high magnetoresistances can be obtained in point contacts due to the existence of constrained domain walls of very small sizes.¹²

These results motivated the present investigation of the role played by geometrically constrained magnetic nanoinhomogeneities. For this purpose, a new concept of nanostructured granular systems was used. The matrix is an electrodeposited polycrystalline Co nanowire of about 100 nm diameter and 50 μm length,¹³ in which pure carbon or carbon-covered Co nanoparticles of well-defined size and shape are embedded. The nanoparticles in the ferromagnetic submicrometric section of the wire play the role of pinning defects for the domain walls. It is shown in this paper that the nature of the resistivity (diffusive versus nondiffusive) is determined by the density of the nanoparticles in the matrix. Above a given value of particle density corresponding to a percolation threshold, the section of the wire is obturated and the transport properties are not diffusive. Below this density,

the resistivity is mainly defined by the conductivity of the Co ferromagnetic matrix. The magnetoresistance is very similar in both cases, suggesting that it is due to the constrained domain walls at the interfaces.

In the following, two kinds of samples corresponding to two types of embedded nanoparticles have been compared. Samples of type A are prepared with magnetic Co particles encapsulated in graphitic carbon shells. The nanoparticles are obtained by an arc discharge technique, and the structural and magnetic properties of the particles have been described in Refs. 14 and 15. Characterization by electron microscopy shows that the particles are mainly monocrystalline and covered by three to five graphitic shells. The mean diameter of the nanoparticles is 13.5 nm in the present case, with a dispersion of about 8 nm [Fig. 1(a)]. The magnetization of a single particle is about 1.8×10^{-15} emu. The blocking temperature is about 300 K, so that the particles do not have a superparamagnetic behavior in the temperature range of the experiment.

Samples of type B are composed of nonmagnetic spheri-

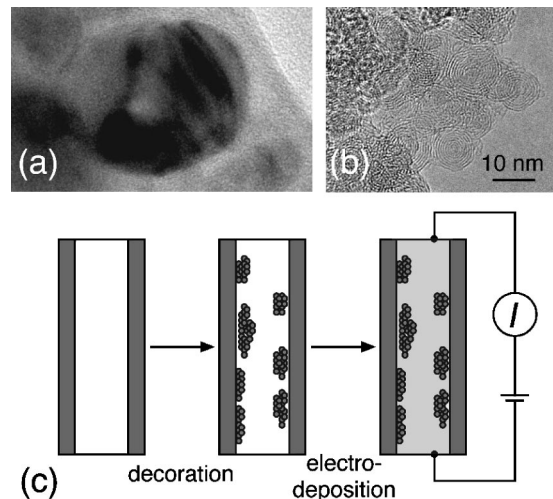


FIG. 1. Transmission electron microscopy micrographs of (a) carbon-encapsulated Co particles (embedded in a Co wire), (b) carbon onions, and (c) fabrication procedure.

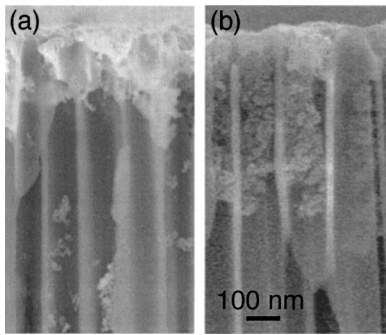


FIG. 2. Scanning electron microscopy micrographs of an aluminum oxide membrane with (a) decorated and (b) obturated pores.

cal carbon nanoparticles, the so-called carbon onions [see Fig. 1(b)] obtained by high-temperature annealing of crystalline nanodiamond particles as described in Ref. 16.

The nanowires are prepared in two main steps [Fig. 1(c)]. First, the pores of an aluminum oxide microfiltration membrane are filled with nanoparticles. The nanoparticles are dispersed in ethanol and sonicated before being driven into the pores by hydrodynamic depression. Second, a metallic Co “cement” is electrodeposited on the pores, and a single nanowire is contacted by a method described in Ref. 17. The obtained nanowires are $l=50\ \mu\text{m}$ long with a diameter of 200 nm (or a section $S=12.5\times 10^{-14}\ \text{m}^2$, $S/l=2.5\times 10^{-8}\ \text{m}$).

Scanning electron microscopy reveals that the particles penetrate inside the pores over a maximum distance of about $1\ \mu\text{m}$ (Fig. 2). Depending on the quantity of particles driven through the membranes, the pores can be either decorated [Fig. 2(a)] or completely obturated [Fig. 2(b)]. Magnetic measurements of the membranes with decorated pores (but without the ferromagnetic cement) show that about 1% of the pore surface in the membrane is occupied by the encapsulated Co nanoparticles, which corroborates the scanning electron microscopy (SEM) measurements.

In order to deduce the magnetoresistance produced by the carbon nanoparticles embedded in the electrodeposited Co matrix, the measurements are compared to the results obtained on a homogeneous Co wire without particles. All measurements are performed with the field perpendicular to the wire axis (except if specified otherwise). The transport and magnetotransport properties of homogeneous Co wires have been studied in detail in previous studies.^{13,18,19} The important point is that the magnetoresistance is due to the anisotropic magnetoresistance (AMR) only. There is hence no significant temperature dependence of the magnetoresistance hysteresis loop [see Fig. 3(a)], except a variation of a few percent due to modification of the magnetic configuration at low field. The amplitude of the AMR signal is due to the difference between the resistance with the magnetization perpendicular to the current (i.e., magnetization along the saturation field, at about 4 T) and the magnetization parallel to the current. The last configuration (magnetization aligned uniformly along the wire axis) is due to the strong shape anisotropy of the wire (aspect ratio about 100) and the relative homogeneity of the nanocrystalline Co. The whole profile is hence very similar for all measured wires.

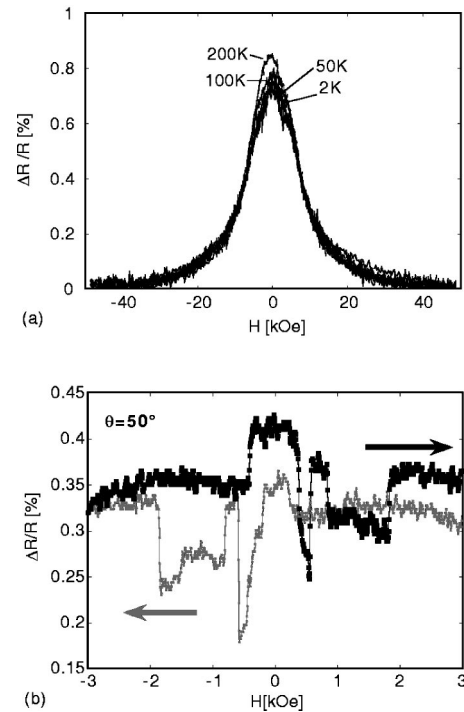


FIG. 3. (a) Magnetoresistance hysteresis loop of a homogeneous Co nanowire at various temperatures. The magnetic field is applied perpendicular to the wire axis. The magnetoresistance is taken as $\Delta R/R = [R(H=0\ \text{kOe}) - R(H=48\ \text{kOe})]/R(H=48\ \text{kOe})$. (b) Close-up of the magnetoresistance of a Co nanowire decorated by Co particles encapsulated in graphitic carbon shells. The magnetic field is applied at 50° with respect to the wire axis.

The general shape of the magnetoresistance hysteresis loop (measured with perpendicular fields) of Co nanowires with carbon-encapsulated Co particles is also rather similar to that of homogeneous Co nanowires. The lowest magnetoresistance, which corresponds to the magnetization perpendicular to the wire axis, is also obtained by applying a field above the saturation field. However, the configuration with the magnetization aligned along the wire axis can no longer be obtained due to magnetic inhomogeneities.

Pinned domain walls reduce the effective magnetization which contributes to the AMR and lead to vortices or extended domain walls at low field. The complexity of the magnetic configurations (vortices or extended domain walls) appears at low field for small angles of the applied field with respect to the wire axis [Fig. 3(b)]. Such complex structures were never observed on single contacted homogeneous wires without nanoparticles. Due to these magnetization states, the AMR hysteresis loop is then expected to be much smaller with the presence of nanoparticles inside the Co matrix. The reproducibility and stability of the samples is excellent and is identical to the samples without nanoparticles.

Below the percolation threshold, when the section of the pores is not obturated, the presence of particles leads to a GMR behavior no matter whether the particles are of type A or B. The GMR behavior is identified by the amplitude and temperature dependence of the effect. The $I(V)$ curves show no significant deviation from Ohm’s law. Figure 4 shows the magnetoresistance hysteresis loop at various temperatures for

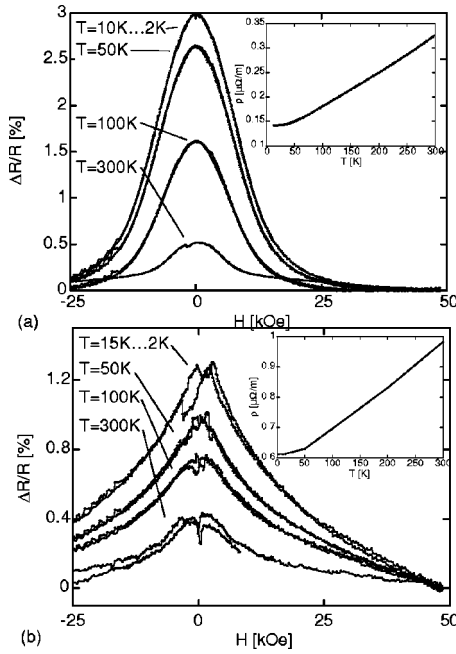


FIG. 4. Magnetoresistance hysteresis loops of a Co nanowire with nanoparticles measured at various temperatures. The field is applied perpendicular to the wire axis. Insets: temperature dependence of the resistivity at zero field. (a) Carbon-encapsulated Co particles and (b) carbon onions.

sample A [C-Co nanoparticles: Fig. 4(a)] and for sample B [carbon onions: Fig. 4(b)]. The anisotropy is reduced or modified with respect to the homogeneous Co wires. The AMR is below 0.5% (measured at 300 K by assuming no GMR contributions), as expected. The MR is enhanced by a factor of about 6 between room temperature and 20 K. The difference in the value of the GMR between samples A and B, typically a factor of 2 here, is probably due to the difference in particle density inside the pores. The GMR is the same decreasing function of the temperatures for both types of samples, with a typical plateau from 2 K up to about 20 K, which coincides more or less with the residual resistivity (inset, Fig. 4). The non-normalized $\Delta R(T)$ follows also the temperature dependence of the GMR. The fact that both samples have a comparable magnetoresistance shows that the nature of the particles (ferromagnetic versus nonferromagnetic) is not directly involved in the spin-flip scattering mechanism. This implies that spin diffusion is located at or near the surface of the particles, and the magnetic configurations (the constrained domain walls) necessary for spin diffusion are due to the presence of the particles.

The GMR of samples of type A are about 3% from 12 K down to 2 K. This value is measured with respect to the resistance of the whole 50 μm wire. Since the particles fill about 1% of the total pore volume, the optimization of the process may lead to some hundreds of a percent of GMR. The possible mechanism involved here is that many conduction channels are in parallel [which can be observed in Fig. 2(a)] and some of them are ballistic. The observed magnetoresistance would result from the strong ballistic magnetore-

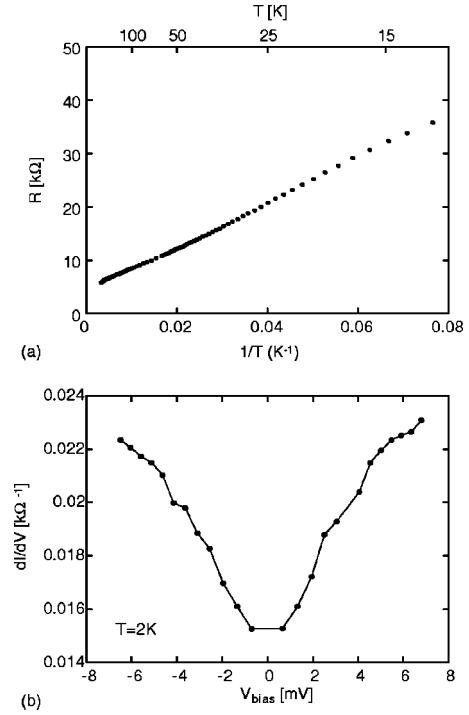


FIG. 5. (a) $1/T$ temperature dependence of the resistance (at zero field) and (b) differential conductance as a function of bias voltage at 2 K.

sistance averaged out with the nonballistic conduction channels in parallel and also summed over many configurations in series.

Above the percolation threshold, when the section of the wire is obturated by the nanoparticles, the value of the resistivity is very high (three orders of magnitude higher than that of decorated pores). The transport mechanism is clearly non-Ohmic as shown by our measurement of the temperature dependence of the resistance and the differential conductance (Fig. 5). The $1/T$ dependence of the resistivity [Fig. 5(a)] was already observed in a compact assembly of carbon onions.²⁰ The $dI/dV(V)$ profile [Fig. 5(b)] can be expected in the case of tunneling magnetoresistance.³ This non-Ohmic profile disappears at about 20 K, and the resistivity remains constant above this temperature.

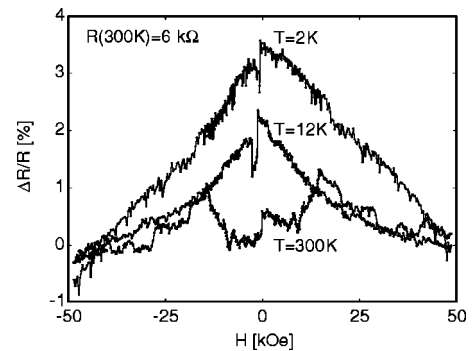


FIG. 6. Magnetoresistance of cobalt ions embedded in a Co nanowire measured at $I = 50$ nA ($V_{\text{bias}} = 2$ mV). The resistance is about $R_0 = 6$ k Ω at $T = 300$ K and $R = 38$ k Ω at 2 K.

The magnetoresistance, Fig. 6, is very similar to that found in the Ohmic regime. A decreasing function of the temperature is also obtained, but without the plateau systematically observed in Ohmic samples below 20 K. Such temperature dependence has been predicted in the framework of a granular tunneling magnetoresistance theory.²¹

The qualification of tunnelinglike magnetoresistance is then suggested by the $dI/dV(V)$ and $R(T)$ curves. However, the hopping magnetoresistance, the ballistic magnetoresistance, or any non-Ohmic resistance with spin-dependent scattering may also account for both temperature dependence and $I(V)$ measurements.²²

In conclusion, we have measured the magnetoresistance properties of carbon nanoparticles embedded in Co nanowires. The nature (magnetic or nonmagnetic) of the embedded nanoparticles plays no qualitative role in the magnetore-

sistance behavior. This result implies that the magnetoresistance properties arise from the magnetic configurations in the vicinity of the nanoparticles, the constrained domain walls, and not from the spin-dependent transport properties through the particles. More surprisingly, although the density of the particles inside the nanowire is a crucial parameter for the electronic transport properties (defining the diffusive to hopping or tunneling crossover), the spin-dependent transport properties (amplitude and shape) are not modified. This study suggests that the magnetoresistance is due to ballistic magnetoresistance (as observed in single ballistic conduction channels^{10,11}), but averaged over many conduction channels.

We are grateful to the Center Interd epartemental de Microscopie Electronique of EPFL (CIME-EPFL) for access to electron microscopy facilities.

*Electronic address: jean-eric.wegrowe@epfl.ch

¹M.N. Baibich, J.M. Broto, A. Fert, F. Nguyen Van Dau, F. Petroff, P. Etienne, G. Creuzet, A. Friederich, and J. Chazelas, *Phys. Rev. Lett.* **61**, 2472 (1988).

²G. Binasch, P. Gr unberg, F. Saurenbach, and W. Zinn, *Phys. Rev. B* **39**, 4828 (1989).

³J.S. Moodera, L.R. Kinder, T.M. Wong, and R. Meservey, *Phys. Rev. Lett.* **74**, 3273 (1995).

⁴A.E. Berkowitz, J.R. Mitchell, M.J. Carey, A.P. Young, S. Zhang, F.E. Spada, F.T. Parker, A. Hutton, and G. Thomas, *Phys. Rev. Lett.* **68**, 3745 (1992).

⁵J.Q. Xiao, J.S. Jiang, and C.L. Chien, *Phys. Rev. Lett.* **68**, 3749 (1992).

⁶J.T. Gittleman, Y. Goldstein, and S. Bozowski, *Phys. Rev. B* **5**, 3609 (1972).

⁷A. Gerber, *Physica B* **280**, 331 (2000); A. Milner, A. Gerber, B. Groisman, M. Karpovsky, and A. Gladkikh, *Phys. Rev. Lett.* **76**, 475 (1996); A. Gerber, A. Milner, B. Groisman, M. Karpovsky, A. Gladkikh, and A. Sulpice, *Phys. Rev. B* **55**, 6446 (1997).

⁸M. Holdenried and H. Micklitz, *Eur. Phys. J. B* **13**, 205 (2000).

⁹S. Rubin, M. Holdenried, and H. Micklitz, *Eur. Phys. J. B* **5**, 23 (1998).

¹⁰N. Garcia, M. Munoz, and Y.W. Zhao, *Phys. Rev. Lett.* **82**, 2923

(1999).

¹¹M. Coey (private communication).

¹²P. Bruno, *Phys. Rev. Lett.* **83**, 2425 (1999).

¹³J.-E. Wegrowe, D. Kelly, A. Franck, S.E. Gilbert, and J.-Ph. Ansermet, *Phys. Rev. Lett.* **82**, 3681 (1999).

¹⁴J.-M. Bonard, A. Sallin, and J.-E. Wegrowe, in *Electronic Properties of Novel Material—Molecular Nanostructures*, edited by Hans Kuzmany, J org Fink, Michael Mehring, and Siegmor Roth, AIP Conf. Proc. No. 544 (AIP, Melville, NY, 2000), p. 508.

¹⁵J.-M. Bonard, S. Seraphin, J.-E. Wegrowe, J. Jiao, and A. Chatelain, *Chem. Phys. Lett.* **343**, 251 (2001).

¹⁶V.L. Kuznetsov, A.L. Chuvilin, Y.V. Butenko, S.V. Stankus, R.A. Khairulin, and A.K. Gutakovskii, *Chem. Phys. Lett.* **289**, 353 (1998).

¹⁷J.-E. Wegrowe, S.E. Gilbert, V. Scarani, D. Kelly, B. Doudin, and J.-Ph. Ansermet, *IEEE Trans. Magn.* **MAG-34**, 903 (1998).

¹⁸J.-E. Wegrowe, A. Comment, Y. Jaccard, J.-Ph. Ansermet, N.M. Dempsey, and J.-P. Nozi eres, *Phys. Rev. B* **61**, 12 216 (2000).

¹⁹U. Ebels, A. Radulescu, Y. Henry, L. Piraux, and K. Ounadjela, *Phys. Rev. Lett.* **84**, 983 (2000).

²⁰J.-P. Salvetat and L. Forr o (unpublished).

²¹J.S. Helman and B. Abeles, *Phys. Rev. Lett.* **37**, 1429 (1976).

²²N. Garcia, *Appl. Phys. Lett.* **77**, 1351 (2000).